ORIGINAL CONTRIBUTION

# Chitosan-based nanocapsules: physical characterization, stability in biological media and capsaicin encapsulation

**Francisco M. Goycoolea · Angela Valle-Gallego · Rossana Stefani · Bianca Menchicchi · Laurent David · Cyrille Rochas · Manuel J. Santander-Ortega · María J. Alonso**

**Abstract** This study addresses the effect of the degree of *N*-acetylation (DA ~1.4–56 %) of chitosan (CS) of low and medium molecular weight ($M_w$~9.5–13.2 and ~122–266 kDa, respectively) on the biophysical properties, colloidal stability and encapsulation efficiency of capsaicin (a lipophilic drug currently used in pain therapy) of CS-based nanocapsules (NCs). The average diameter of the NCs varied within the range of ~150–200 nm, but it was slightly higher for NCs comprising high $M_w$ CS than for those with low $M_w$ CS. The zeta potential ($\zeta$) was highly positive and clearly dependent on the $M_w$ of CS, exhibiting a monotonic decreasing trend concomitant with the increase in DA. Both results suggest that $M_w$ and DA of CS have an effect on the disposition of the polysaccharide onto the phospholipidic surface. Synchrotron SAXS studies revealed a monotonic increase in Bragg interplanar distances (from ~55 up to ~67 Å) as a function of the DA, a finding that agrees with previous results that are consistent with the capacity of hydrophobic domains to disturb the crystalline state of gelled phospholipidic membranes. Colloidal stability studies carried out in cell-culture biological media revealed the determinant role of hydration forces, a short-range repulsive interaction, on the stability of the NCs. Finally, $M_w$ and DA of CS both influenced the encapsulation efficiency of capsaicin, thus showing the effect of the harnessed NCs shell on its capacity to encapsulate lipophilic drugs.

**Keywords** Capsaicin · Chitosan · Nanocapsules · Synchrotron SAXS · Stability

## Introduction

Colloidal nanocapsules (NCs) comprised by an oily core, lecithin and a hydrophilic coat of chitosan (CS), a natural aminopolysaccharide, have been one of the systems at the focus of research due to their promising potential as an effective drug delivery platform for transmucosal administration of

F. M. Goycoolea · A. Valle-Gallego · B. Menchicchi · M. J. Santander-Ortega · M. J. Alonso
Department of Pharmacy and Pharmaceutical Technology,
Universidad de Santiago Compostela,
Campus Sur s/n,
15782 Santiago de Compostela, Spain

R. Stefani
Dipartimento di Chimica e Tecnologie,
Farmaceutiche ed Alimentari,
via Brigata Salerno 13,
16147 Genova, Italy

M. J. Santander-Ortega
Department of Pharmaceutical and Biological Chemistry,
UCL School of Pharmacy, University College London,
WC1N 1AX,
London, UK

L. David
Laboratoire des Matériaux Polymères et des Biomatériaux,
UMR CNRS 5223, Ingénierie des Matériaux Polymères (IMP),
Université Lyon 1, Université de Lyon,
15 Boulevard A. Latarjet, Bâtiment ISTIL,
69622 Villeurbanne Cedex, France

C. Rochas
CERMAV-CNRS,
BP53, 38041 Grenoble, France

F. M. Goycoolea (✉)
Institut für Biologie und Biotechnologie der Pflanzen,
Westfälische Wilhelms-Universtät Münster,
Schlossgarten 3,
48149 Münster, Germany
e-mail: goycoole@wwu.de

peptides, lipophilic drugs and vaccines [1–6]. The driving physicochemical mechanism whereby these systems self-assemble is by spontaneous emulsification, also regarded as "solvent displacement" [7], whereby a homogeneous liquid–liquid nucleation occurs as acetone and ethanol, initially admixed in the organic phase, migrate to the aqueous phase, yielding an oil and water (o/w) nanoemulsion stabilized by the surfactant (lecithin) adsorbed at the o/w interface. Either during its formation or in a subsequent incubation step, a water-soluble polymer can be incorporated as a coat that interacts with the phospholipids of lecithin, thus, effectively, yielding a core–shell colloidal nanocapsule structure.

The rationale for the design of new nanocarrier systems, such as oily core nanocapsules and matrix nanospheres, has been to exert control, not only the size but also on the surface properties and composition of these systems, so that the stability in biological fluids and interaction with mucosal surfaces can be adapted to achieve a satisfactory transmucosal drug delivery. In this regards, the hypothesis is that CS significantly improves the ability of NCs to deliver drugs, such as biologically active peptides (e.g. salmon calcitonine (sCT)), across the corneal, nasal and oral mucosae [1–4]. Other proof-of-principle studies have revealed that these systems are useful for the intracellular transport of lipophilic drugs, such as docetaxel, a well-established anti-mitotic drug used primarily for the treatment of breast, ovarian and non-small cell lung cancer [5]. Also, this nanocapsule system has been shown to be an effective delivery vehicle for the intranasal administering of vaccines such as hepatitis B surface antigen [6].

High-purity biomedical-grade CS is available either as the neutral polymer or in different salt forms (typically as the hydrochloride or glutamate salts) and at varying $M_w$ and degree of acetylation (DA). Hence, previous studies have addressed the role of these characteristics on the physical properties of NCs [1, 3], stability and drug encapsulation efficiency. In general, an increase in CS's $M_w$ leads to NCs of larger size and to a slight elevation in $\zeta$, while CS's salt form has no discernible effect on these parameters. By contrast, neither CS's salt form nor $M_w$ (in the range 160–450 kDa) have a significant effect on both the viability or the transepithelial electrical resistance of Caco-2 cell monolayers [3]. Meanwhile, in the same study, it was found that the presence of the CS coat was necessary for the capacity of NCs to achieve a significant pharmacological hypocalcemic response after oral administration of sCT-loaded NCs to rats. The $M_w$ of CS had no effect in this response.

A previous work [8] addressed the impact of the CS's DA and $M_w$ on the stability of different chitosan NCs. The stability of these systems under physiological conditions seemed not to be controlled neither by the classical electrostatic (repulsive) nor the van der Waals (attractive) DLVO (Derjaguin, Landau, Verwey and Overbeek) potentials of interaction but rather by short-range repulsive hydration forces. Both CS's $M_w$ and DA had a clear effect on the organization of the polysaccharide at the NC's shell. While low $M_w$ and high DA promoted more efficient packing, high $M_w$ and low DA led to more heterogeneous distribution of the CS's molecules.

In the present study, we have addressed the role of the DA on the physical properties and stability on biological fluids of CS NCs. To this end, the lower limit of $M_w$ of CS of previous studies was extended to ~10 kDa while using the neutral form of CS dissolved in stoichiometric amounts of acetic acid. From the influence of CS's DA and $M_w$ on the zeta potential and the particle size of the nanocapsules along with synchrotron SAXS measurements, we propose a model to account for the way in which CS organizes at the NC's surface. This model has helped us to understand the role of the CS's physicochemical properties on the colloidal stability displayed by the NCs under physiological conditions. For selected NC systems, we have also studied the capacity to associate capsaicin (8-methyl-*N*-vanillyl-6-nonenamide), a lipophilic drug, in the oily core. Capsaicin, the pungent vanilloid found in hot chilli peppers, is approved as a drug for the treatment of chronic pains (e.g. arthritis, migraine, diabetic neuropathy) [9, 10]. In light of this, identifying new potential nanocarriers for intracellular, transdermal and/or for intranasal delivery of capsaicin, so as to regulate the activity of its receptors (TRPV1 receptors) in various tissues, appeals as a potential emerging therapeutic strategy.

## Results

### Chitosan samples characteristics

Table 1 shows the physicochemical characteristics of the CS samples utilized in this study to prepare NCs. This set of samples spans a wide range of $M_w$ (~10 to ~279 kDa) and degree of acetylation (DA 1.4 to 56 %). Along with the degree of polymerization ($M_w$), the DA is a critical parameter that directly determines the physicochemical and biological properties of chitosan and the materials derived from it.

### Nanocapsule characterization

*Z-average size* Figure 1 shows the dependence of Z-average diameter of the various NC systems comprising CS samples of varying DA and $M_w$. Notice in Fig. 1 that HDP CS-based NCs had a Z-average diameter in the range ~175–219 nm (polydispersity index, PDI~0.14–0.19). In turn, LDP CS systems exhibited slightly lower Z-average sizes than those of HDP CS NCs (diameter ~127–158 nm; PDI~0.13–0.21) for CS with DA 1.2 % to 27.8 % whereas, for LDP-DA51, the size was significantly greater (~189±12 nm). In general,

**Table 1** Physicochemical characteristics of chitosan samples

| Chitosan sample | Degree of *N*-acetylation (%) | $M_w$ | $M_n$ | $I_p$ | DP[d] |
|---|---|---|---|---|---|
| HDP-DA1 | 1.6[a] | 123900[c] | 89000[c] | 1.39[c] | 766 |
| HDP-DA11 | 11.0[a] | 122100[c] | 75330[c] | 1.62[c] | 737 |
| HDP-DA27 | 27.5[a] | 143000[c] | 85710[c] | 1.67[c] | 818 |
| HDP-DA56 | 56.0[a] | 266100[c] | 139700[c] | 1.90[c] | 1442 |
| LDP-DA1 | 1.4[a] | 13200[c] | 11130[c] | 1.19[c] | 82 |
| LDP-DA9 | 9.2[a] | 9572[c] | 5914[c] | 1.62[c] | 58 |
| LDP-DA27 | 27.8[a] | 11530[c] | 8120[c] | 1.42[c] | 67 |
| LDP-DA51 | 51.0[a] | 11420[c] | 6012[c] | 1.90[c] | 63 |
| ChitopharmS® | 20.0[b] | 279200[b] | 97100[b] | 2.88[b] | 1648 |

[a] Degree of acetylation as determined by $^1$H NMR spectroscopy

[b] Data in accordance with specifications given by supplier

[c] Parameters determined by GPC-HPLC with multidetection (MALLS-DRI): weight average molecular weight ($M_w$); number average molecular weight ($M_n$); polydispersity index ($I_p = M_w/M_n$)

[d] Degree of polymerization (DP = $M_w$/molar mass per residue)

the PDI values, derived from the second cumulant of the fitted decay autocorrelation function, were small (<~0.21) and could be fitted by monomodal size distribution curves for all systems. Notice that LDP-DA51-coated NCs exhibited a greater size than the rest of particles coated with LDP CS of DA 1.4–27.5 %. The increment in size is not as marked for HDP-DA56-coated as for LDP-DA51 NCs. In turn, naked nanoemulsions without CS had a Z-average size of 151±2 nm.

*Zeta potential (ζ)* By contrast with the variations observed in NCs' average size with DA, ζ values decreased under a non-linear monotonic dependence with increasing DA for both LDP CS and HDP CS NCs (Fig. 2). For systems comprising LDP CS, ζ decreased from +39 to +26 mV (i.e. 33 % reduction) while for HDP CS ones, it descended from +47 to +36 mV (i.e. 23 % reduction). This is rationalized as the consequence of the reduction in CS's positive charge density due to the decrease in DA. In both cases, a linear negative dependence was observed for DA≥~9 %. Overall, LDP-based systems exhibited slightly less positive ζ values than did systems comprising HDP CS.

*Chitosan association* A separate experiment aimed to evaluate the association of CS to the NCs. The results revealed that regardless of CS's $M_w$ and DA, almost the full amount of added polysaccharide (>96.8 %) incorporated into the NCs (Fig. 3).

*Transmission electron microscopy* The nanocapsules consistently exhibited a spherical morphology, as unequivocally visualized by transmission electron microscopy (TEM) for representative systems (Fig. 4). In general, the CS NCs (Fig. 4a–e) exhibited a smoother surface than did the nanoemulsion (Fig. 4f). The size of the various imaged NCs lay within the expected range as determined by photocorrelation spectroscopy-non-invasive backscattering (PCS-NIBS). Interestingly, a close inspection of the TEM images reveals the presence of a core–shell structure on the various NCs as well as in nanoemulsion particles (Fig. 4f). Finer aspects of the surface topology than these either lie below TEM spatial resolution (~4–5 nm) or could not be imaged due to poor contrast.

*Synchrotron SAXS measurements* Figure 5a shows Synchrotron SAXS scattering curves for NCs comprising CS of

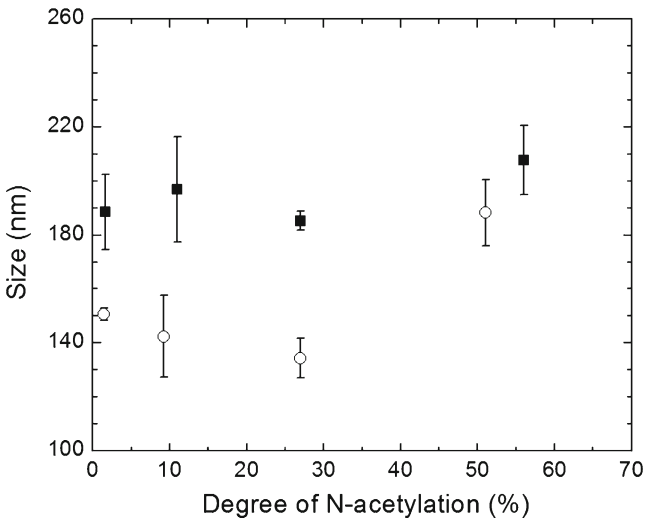


**Fig. 1** Effect of the variation of the degree of *N*-acetylation of chitosan on the Z-average size (diameter) of nanocapsules comprising HDP (*filled square*) or LDP (*empty circle*) chitosan (water at 25 °C; mean±SD; $n=3$)

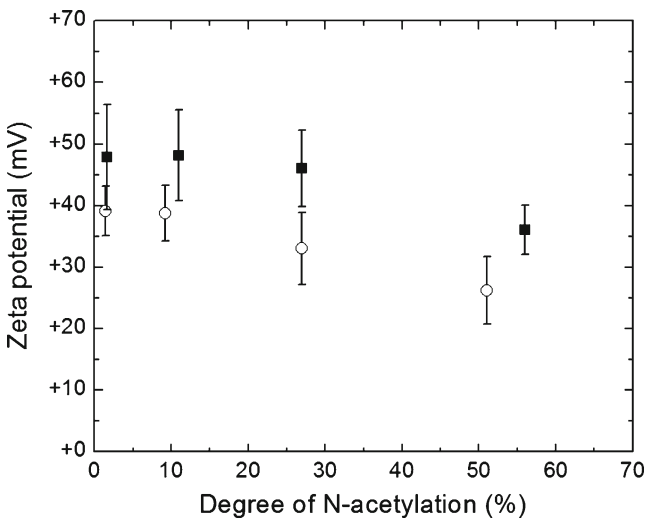


**Fig. 2** Effect of the variation of the degree of *N*-acetylation of chitosan on the zeta potential (ζ) of nanocapsules comprising HDP (*filled square*) or LDP (*empty circle*) chitosan (NaCl 1 mM at 25 °C; mean±SD; $n=3$)

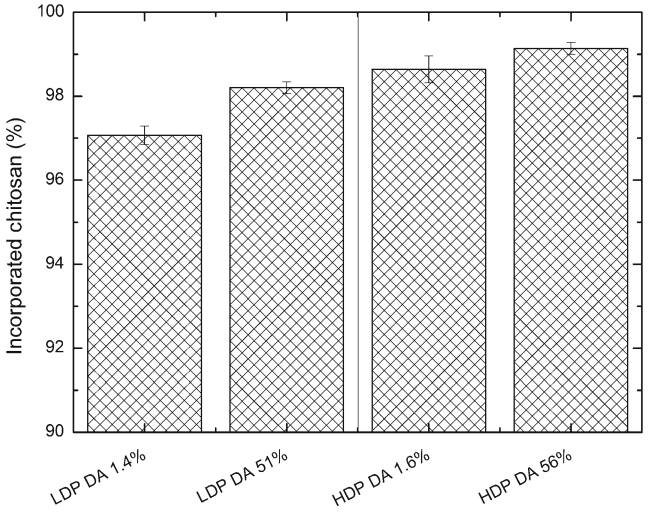


**Fig. 3** Estimated amount (%) of chitosan adsorbed at the nanocapsules with respect to the initially added concentration (0.5 mg/mL; mean ±SD; $n$=3)

varying DA of low and high $M_w$ along with the nanoemuslion free of CS. Notice that, in all the intensity curves for NCs, well-defined Bragg diffraction peaks appear at scattering vector ($q$) values in the range ~0.08 to ~0.11 Å$^{-1}$ that correspond with interplanar spacing distances ($d$=2π/$q$) that lie within a narrow range of magnitude ($d$ ~55 to ~66 Å). Figure 5b illustrates the dependence of $d$ with the DA of the various CS samples. Clearly, $d$ values show a non-linear monotonical elevation as the DA increases, irrespectively of CS's $M_w$.

## Stability in biological media

The stability of NCs during incubation in minimum essential medium (MEM), endothelial cell growth medium (ECGM), and Roswell Park Memorial Institute medium formulation-1640 (RPMI-1640) cell culture media, in all cases, supplemented with fetal calf serum and other essential nutrients and necessary components, was studied from the evolution of the particle size distribution as probed by dynamic light scattering (PCS-NIBS) at varying time intervals up to 48 h at 37 °C. MEM and RPMI are both used for the cultivation of human cell lines that grow either adhered as monolayers or in suspension, such as normal and neoplastic leukocytes, including fresh lymphocytes and dendritic cells, while ECGM is the commonly used medium to cultivate endothelial cells (e.g. HUVEC). Figure 6 illustrates the time evolution of the particle size distribution curves for typical curves of LDP CS- and HDP CS-based NCs during incubation in supplemented MEM (pH ~7.4) of low (Fig. 6a, c) or high (Fig. 6b, d) DA. The rest of the tested NCs in MEM had remarkably similar curves to those shown in Fig. 6b–d. The inspection of the plots reveals that, in general, essentially similar Gaussian monomodal size distribution curves described the behaviour of all NC systems regardless of the type of CS. With the exception of HDP-DA1 NCs (Fig. 6c), whose plots appeared shifted towards greater values, the rest of the NCs had similar size distributions. Also, a population of NCs of slightly smaller size appeared after 24 and up to 48 h. Under an identical protocol, NCs were also incubated in ECGM and RPMI-1640 cell culture media. Figure 7 shows the kinetics of the evolution of the Z-average size during incubation in these two media. It can be appreciated that the time evolution of the size of both LDP and HDP CS-coated NCs in ECGM (Fig. 7a, c) depended clearly on CS's DA. In this same medium, NCs comprising LDP or HDP CS of low DA in both cases did show a monotonic increase in size at early incubation times. The elevation in size, however, was modest and not accompanied by an appreciable aggregation process. In turn, systems comprising CS of high DA (≥27 %), even when they had overall lower ζ values, were remarkably stable, with virtually no change in particle size during incubation. By contrast with the results observed in ECGM (and MEM too), in RPMI-1640, the NCs were much less stable, particularly those comprising HDP CS of low DA. In fact, NCs containing HDP-DA1 aggregated immediately upon incorporation into the medium. Notice in Fig. 7d that NCs comprising HDP-DA11 attained particle sizes larger than 1 μm after 200 min and continued increasing beyond this time. For LDP CS (Fig. 7b), the increase in particle size was also evident for CS of low DA (DA~1.4 and 9 %), though these systems did not experience visible aggregation.

## Drug encapsulation

Capsaicin loaded effectively into NCs comprising LDP-DA1 and LDP-DA51 and commercial CS (ChitopharmS® $M_w$ ~280 kDa; DA ~20 %). Loading of capsaicin to a total 2 % did not have a significant influence on the Z-average size, PDI, or on ζ values of any of the NC formulations as shown in Table 2. The encapsulation efficiency (EE) of capsaicin in the tested formulations was high and varied in the range ~60–96 % (Table 2). Interestingly, the highest EE was for systems comprising LDP-DA51 CS whilst slightly lower in systems formulated with ChitopharmS® of much higher $M_w$. Meanwhile, the lowest capacity of capsaicin association was for the systems comprising low $M_w$ of DA 1.4 %. The observed differences in the capacity of NCs to encapsulate capsaicin can be accounted for on the basis of the differences CS's $M_w$ and DA.

The overall high capsaicin encapsulation efficiency achieved coincides well with that observed in previous studies with other liposoluble drugs, such as diazepam [1] or docetaxel [5] for which the reservoir structure of the NCs allowed to encapsulate the drugs with efficiencies of >90 % and 72 %, respectively.

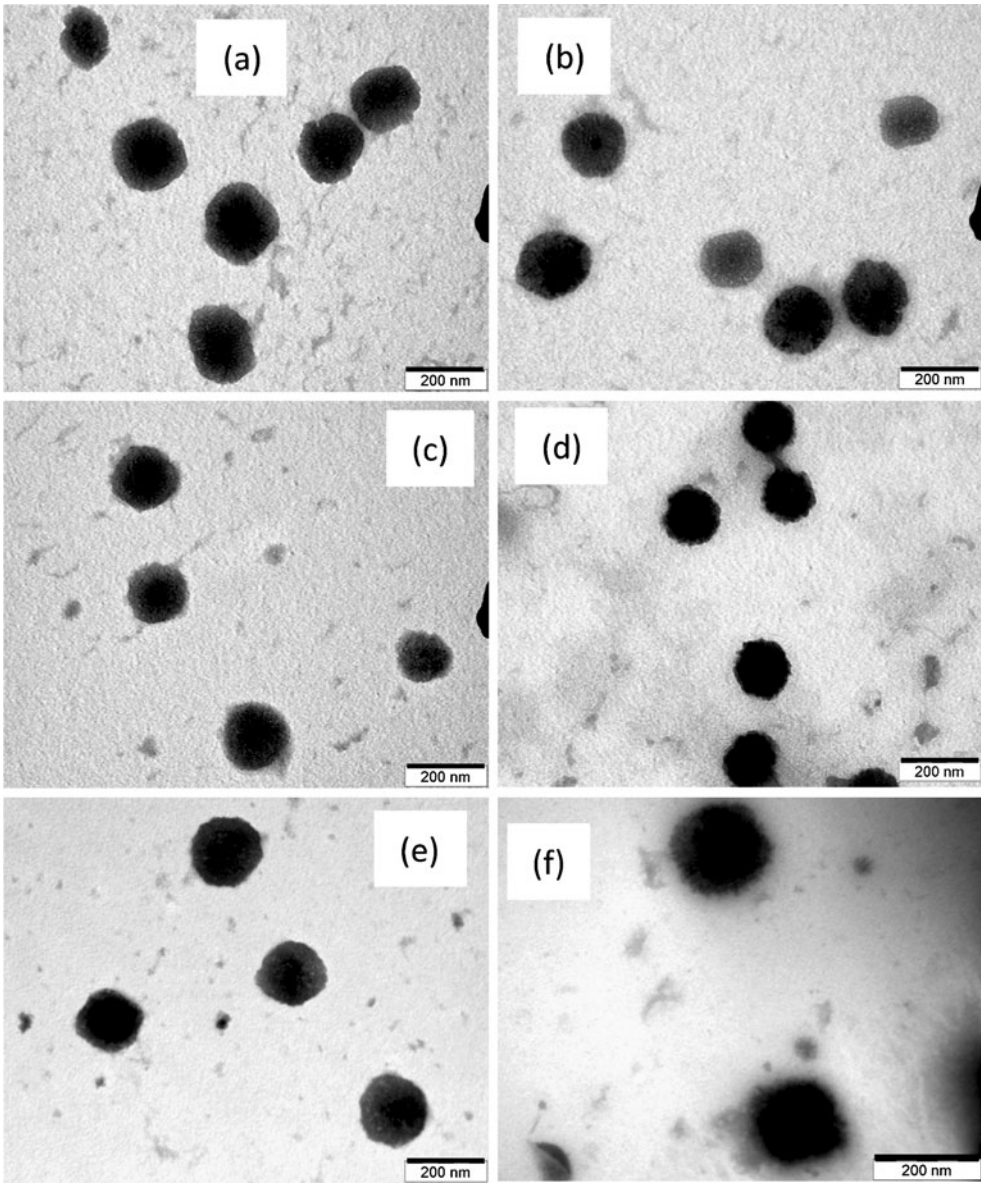


**Fig. 4** Transmission electron microscopy (TEM) images of nanocapsules comprising the following chitosan types: **a** LDP-DA1; **b** LDP-DA51; **c** HDP-DA1.6; **d** HDP-DA11; **e** ChitopharmS® and **f** nanoemulsion. Magnification as shown in *bars*

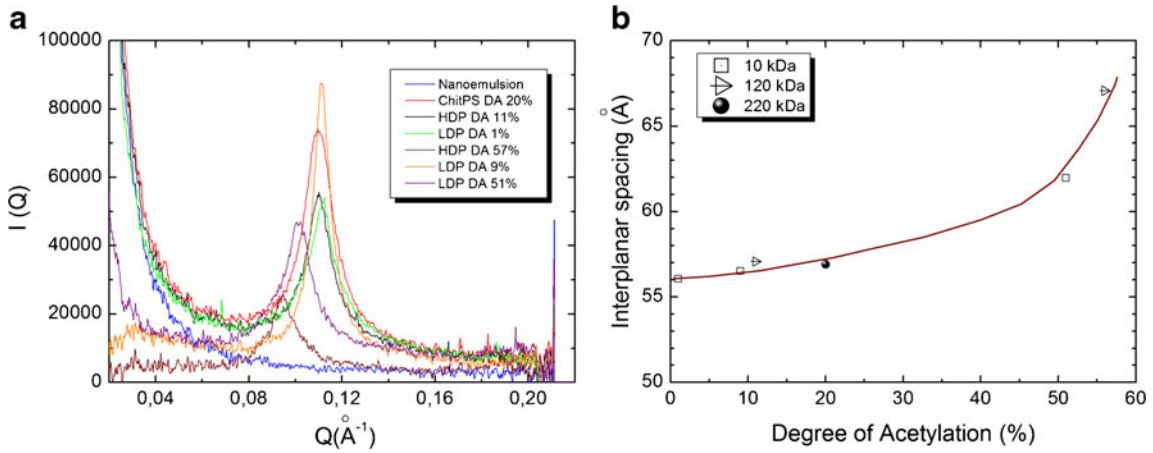


**Fig. 5** **a** SAXS intensity scattering curves for nanoemulsion and nanocapsules coated with chitosan of varying degree of acetylation and $M_w$ (as shown in *label*). **b** Interplanar spacing as a function of the degree of acetylation of chitosans of varying molecular weight (as shown in *label*)

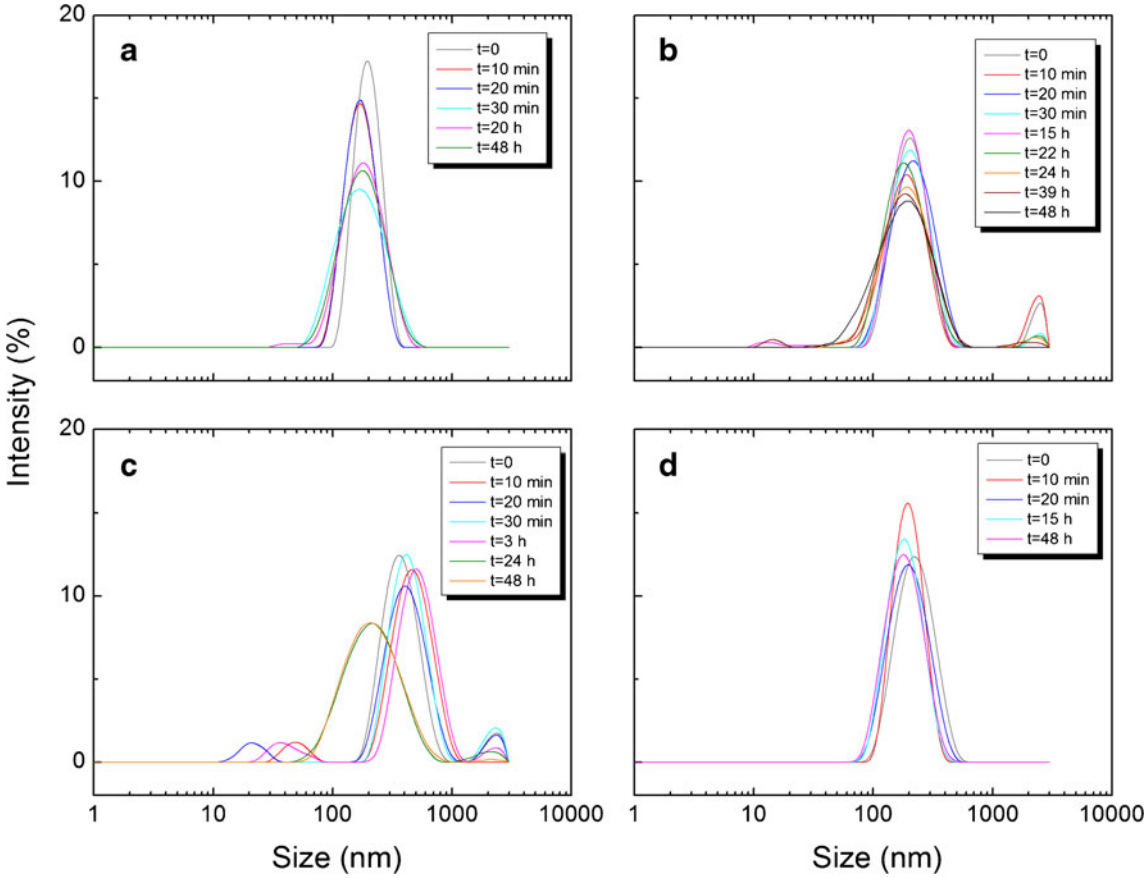


**Fig. 6** Time evolution of the size (diameter) distribution curves of nanocapsules incubated (37 °C) in MEM culture medium for nanocapsules comprising the following chitosan types: **a** LDP-DA1; **b** LDP-DA51; **c** HDP-DA1 and **d** HDP-DA56

## Discussion

Understanding of nanocapsules structure at the molecular level allows not only to chose the optimal lipidic core according with the desired delivery necessities, but also the election of the appropriate coating to achieve the best performance as a function of the administration route and/or target. The recent studies carried out in our lab have demonstrated the potential of CS as polysaccharide shell of lipidic nanocapsules for the transmucosal (e.g. oral and nasal) administration of peptides, anticancer lipophilic drugs and vaccines [2–6, 11, 12]. In spite of the positive results accounting for the use of CS-based NCs as transmucosal drug carriers, successful development of new systems would benefit from a better understanding of the role of CS physicochemical properties on the interaction of the particles with their environment under conditions that resemble those that occur in vivo. Indeed, depending on CS properties, interactions of NCs with electrolytes, proteins and other macromolecules can lead either to the colloidal stabilization of the formulation or else to their aggregation [8]. Based on this, the aim of this work was to examine the effect of CS's DA and $M_w$ on the physical properties, colloidal stability under physiological conditions and capsaicin, a model lipophilic drug, encapsulation capacity of the formulated NCs.

Quantification of the incorporation of CS onto NC's surface has shown that, with no dependence on its DA or $M_w$, more than 90 % of the added CS associated to the NCs. A deeper analysis of these results showed that the increase of CS's DA, that is, of its hydrophobic nature, led to higher incorporation of this polysaccharide to the particles (Fig. 3). This suggests that, although electrostatic attraction is the main force controlling the incorporation of this polysaccharide to the particle, hydrophobic interactions between hydrophobic moieties of CS and hydrophobic patches on the lipidic nucleus also favour the association of this polysaccharide. This suggestion agrees well with the explanation to results previously obtained in large and giant unilamellar vesicles coated with CS [13].

Systems formulated with HDP CS had higher average sizes than the ones formulated with LDP CS. Recent studies showed that CS's $M_w$ does not only affect the overall thickness of the coating shell itself, but it also entails differences in the way CS organizes itself at the NC's surface [8]. Shorter chains of LDP CS are expected to pack themselves more densely as a consequence of a flatter organization of

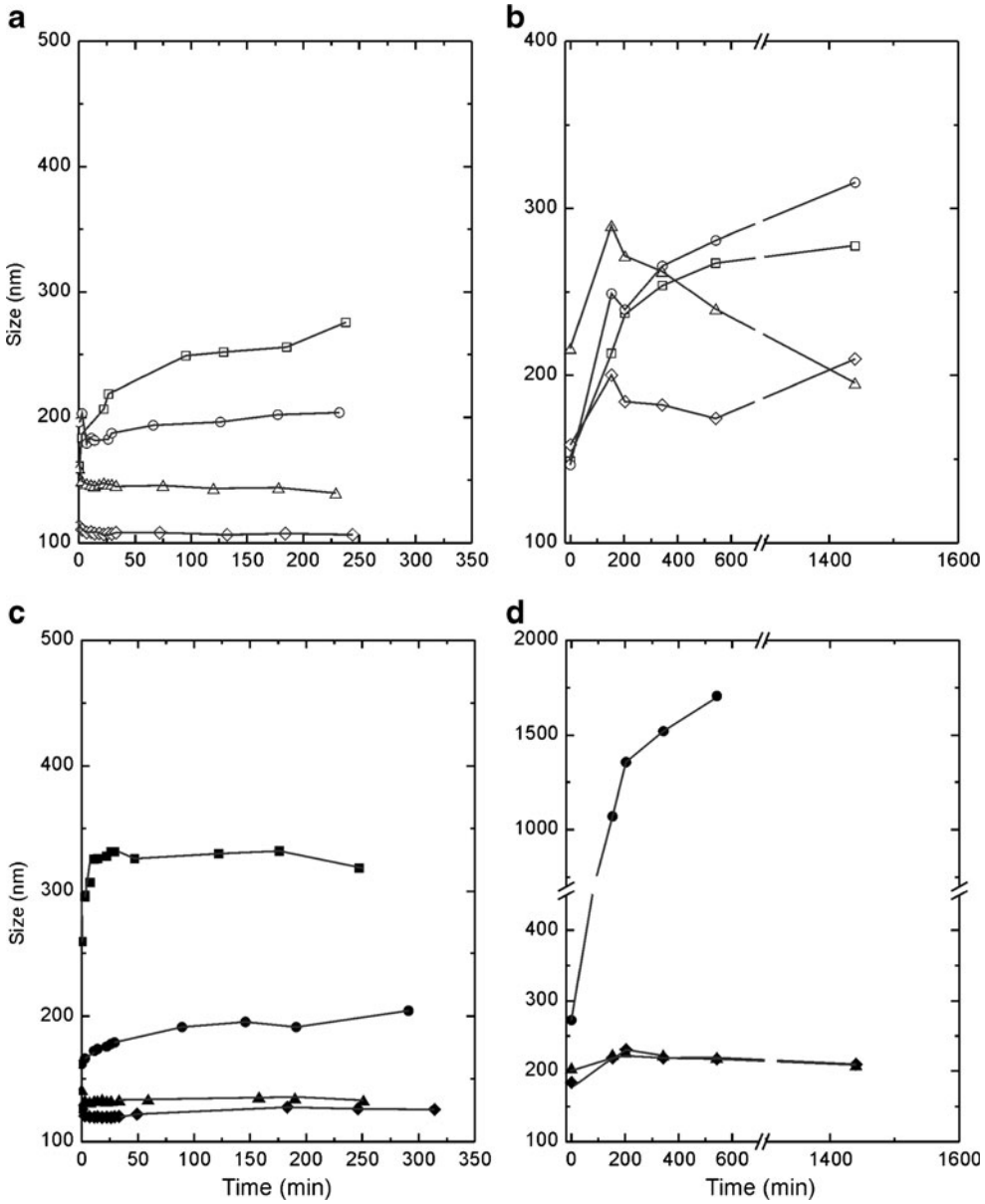


**Fig. 7** Variation of the Z-average size (diameter) during incubation in ECGM (**a** and **c**) or RPMI (**b** and **d**) at 37 °C of chitosan nanocapsules comprising LDP (**a** and **b**) or HDP (**c** and **d**) chitosan of degrees of *N*-acetylation (%) as follows—1.4 (*empty square*), 1.6 (*filled square*), 9.0 (*empty circle*), 11.0 (*filled circle*), 27.8 (*empty triangle*), 27.5 (*filled triangle*), 51.0 (*empty diamond*) or 56.0 (*filled diamond*)

greater cooperativity than that attained by longer chains of HDP CS, presumably due to an entropic disadvantage associated to the local confinement of larger polymer stretches at the NC's surface.

Close inspection of TEM images (Fig. 4) revealed that, although subtle variations in contrast exist between the core and the shell structure of the different NCs, it is difficult to account for these in terms of the suspected presence of flat or coiled patterns of adsorption of CS of varying DA and $M_w$. Moreover, conventional TEM images, in contrast with those obtained by cryo-TEM techniques, may not reveal detailed features the hydrated state of the NC's surface due to drying and shrinkage during the fixation procedure [14].

It was somewhat surprising, in fact, to note that LDP-DA51 NCs exhibited greater size than the rest of particles with LDP CS of DA 1.4–27.5 %. Superficial charge of the nanocapsule is the main force that allows the formation of colloidally stable particles. From electrokinetic characterization of these particles, it is clear that those nanocapsules formulated with LDP CS at the highest DA (LDP-DA51) presented the lowest $\zeta$. Hence, a possible explanation of the observed larger size is the coalescence of the early lipidic droplets coated with LDP CS during the nanocapsule formation to produce vesicles with larger surface and thus with enough number of superficial amino groups able to electrostatically stabilize the nanocapsule. This is in agreement with previous studies conducted on CS-based NCs [1] and in CS "decorated" lipid unilamellar vesicles (LUVs) [13, 15]. It is also diagnostic evidence that CS forms a polycationic coat around the core–shell nanoemulsion, hence forming a true nanocapsule structure. Indeed, nanoemulsions exhibit an extremely negative zeta potential ($\zeta \sim -54 \pm$

**Table 2** Physical characteristics of blank (unloaded) and capsaicin-loaded (2 % load) nanocapsules ($n$=3)

| Formulation | Size (nm) | PDI | ζ (mV) | Capsaicin EE (%)[a] |
|---|---|---|---|---|
| LDP-DA1 blank | 151±2 | 0.12 | +43.6±0.6 | – |
| LDP-DA1 loaded | 155±2 | 0.12 | +54.3±0.6 | 65.8±5.9 |
| LDP-DA51 blank | 188±12 | 0.11 | +28.7±0.3 | – |
| LDP-DA51 loaded | 192±3 | 0.07 | +36.0±0.6 | 95.4±1.3 |
| ChitopharmS® blank | 289±6 | 0.29 | +50.8±1.4 | – |
| ChitopharmS® loaded | 290±5 | 0.34 | +50.7±0.5 | 90.8±0.9 |

[a] Capsaicin's encapsulation efficiency given by $EE$=[(Total capsaicin−Free capsaicin)/Total capsaicin]×100

1 mV) that, upon coating with CS, experiences a marked inversion from highly negative to highly positive ζ values, a result which is consistent with the notion that CS occurs primarily at the nanocapsules' surface [1].

Differences in ζ dependence on DA among the various NCs prepared with LDP CS or HDP CS may be the result of the local organization of CS chains around the NC's shell. In the case of LDP CS of low DA, short, highly charged stiff polymeric chains can be envisaged to pack themselves more closely at the lecithin oil–water interface, thus effectively, leading to an overall greater charge neutralization of phospholipid negative charges. A more uniform distribution of LDP CS than HDP CS can also account for the overall lower ζ values found in LDP CS. This interpretation is also in agreement with a flat, hence compact, arrangement of LDP CS at the NC's surface, as recently proposed for the adsorption of CS on LUVs [13, 15]. Two distinct regimes of behaviour described the dependence of ζ on the proportion of CS coverage for CSs of 50 or 500 kDa. As suggested in such studies, at low degrees of CS coverage, the ζ of the LUVs exhibited no dependence on $M_w$, the consequence of a "flat-like" adsorption of CS chains regardless of their size. While at high degrees of coverage, LUVs coated with high $M_w$ CS showed overall larger ζ values. This behaviour can be attributed to the formation of loops by the high $M_w$ polymer, in agreement with our own interpretations to the differences in size and ζ found between NCs with LDP CS or HDP CS NCs given above.

Interestingly, for both LDP CS- and HDP CS-based systems, the decrease in ζ values is not proportional to the increase in DA, and they only decrease significantly at high DA (>27 %), a phenomenon that can be explained due to the formation of hydrophobic domains that may also perturb the phospholipids interface. The fact that the increase in CS's DA does not accompany a direct reduction in ζ values could be attributed to the preferential distribution of charged amino groups of CS at the NC's surface. This assumption essentially agrees with previous studies addressing the interaction of chitosan with phospholipid bilayers that have suggested that the interaction of CS with diphosphatidyl choline (DPPC) mica-supported membranes leads to a reconstruction of the supported membrane. A gel-state bilayer with a crystalline like structure has been proposed to occur in chitosan–DPPC biomembranes. It has been suggested that chitosan aggregation occurs upon adsorption across the membrane surface. The existence of such aggregates could protect the more neutral, hence hydrophobic, CS stretches, from being exposed to the aqueous phase [16–18]. Synchrotron SAXS studies have addressed, in detail, aspects of the ultrastructure of chitosan-based NCs systems. The origin of Bragg diffractions observed in NCs may lie in the existence of a gel-state layer with a crystalline-like structure that is formed between the phospholipidic interface and adsorbed CS chains, an explanation that agrees with the general interpretations to results obtained in chitosan–DPPC biomembranes probed by atomic force microscopy [16]. The SAXS results are in good keeping with the notion that the adsorption of CS at the NC's surface influences the local organization and molecular architecture of the oil–lecithin–water interface. One can argue that the overall magnitude of the lateral periodic spacings in the crystalline-like bilayer (i.e. Bragg diffraction peaks) increases under a well-defined monotonic trend as so does CS's DA, and irrespective of its $M_w$. The overall magnitude of this effect is ~10 Å (i.e. from $d$~55 to ~66 Å), which lies well within the expected distance range for lecithin polar heads and chitosan layer at the NC's surface [16, 19]. Therefore, it seems reasonable to suggest that the hydrophobic behaviour of CS, which in itself predominates with increasing DA, is important in this regards. The fact that CSs of high DA (DA~51–56 %), with nearly half as much uncharged residues adsorbed slightly better than did the almost fully charged polymers (DA~1.4–1.6 %) (Fig. 3), is in full agreement with this interpretation. CS adsorption to the NC's surface is bound to occur predominantly as a result of electrostatic interactions between oppositely charged $-NH_3^+$ groups in CS and phospholipidic polar heads of lecithin at the lipidic core surface, however, other mechanisms such as hydrophobic interactions may be at play not only in favouring the incorporation of CS but also governing the local organization of CS at the NC's surface [8, 20]. A schematic model in Fig. 8 between CS and the lecithin phospholipid polar heads at the NC's surface illustrates the envisaged local interactions at the NC's surface.

Results from the stability studies in cell culture media revealed that, in general, the NCs were very stable, especially when compared with CS-based nanoparticle systems prepared by ionotropic gelation [21]. This set of experiments allowed the conclusion that CS-based NCs were remarkably stable during incubation in MEM for up to 48 h and ECGM for up to 4 h. It is fair to note that, despite the fact that the pH of fresh MEM and ECGM (pH ~7.45) culture media is well above CS's $pK_o$ (~6.0–7.0) and hence its amino groups are likely to

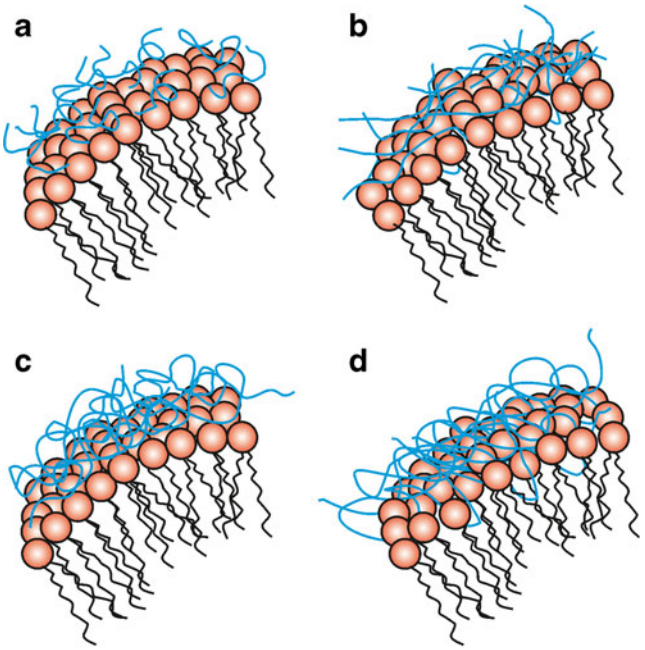


**Fig. 8** Schematic models for the interaction of chitosan and lecithin at the nanocapsule surface as: **a** LDP chitosan of low degree of *N*-acetylation; **b** LDP chitosan of high degree of *N*-acetylation; **c** HDP chitosan of low degree of *N*-acetylation and **d** HDP chitosan of high degree of *N*-acetylation

be almost entirely neutralized [8, 20], the integrity of the NCs persists during prolonged times (e.g. during up to 48 h in MEM). Colloidal stability displayed by these systems at high salt concentrations cannot be explained neither by DLVO theory nor steric hindrance [22, 23]. In this case, the hydrophilic nature of CS originates another stabilization mechanism based on short-range repulsive hydration forces. Such hydration forces become significant when a large number of hydrated ions are accumulated in the proximity of the hydrophilic surface of the nanocapsules [8, 24]. Intensity of hydration forces depends on the CS's conformation and therefore can be modulated as a function of CS's $M_w$ and DA [8]. We have previously demonstrated that low degrees of polymerization and high degrees of acetylation encourage the creation of more uniform polysaccharide shell onto the lipidic core. This leads to the formation of nanocapsules with a more hydrophilic shell, which produces more intense repulsive hydration forces [8]. This explanation agrees well with the lower stability displayed by the HDP systems with low DA compare with the less-charged NCs formulated with CSs of LDP and high DA. Although the former presented much higher surface charge ($\zeta$~+50 mV) compared with the latter ($\zeta$~+40 mV), CS's conformation was the less hydrophilic and then the less apt to promote the colloidal stabilization of the formulation at high ionic strength due to the short-range repulsive hydration forces [8].

An explanation of the markedly characteristic stability exhibited by the NCs in MEM, ECGM and RPMI-1640 is that, although the three media share roughly equivalent composition in terms of salts, amino acids and vitamins, there are subtle differences in the concentration and type of the individual components of their formulation. Indeed, RPMI-1640 contains fivefold greater concentration of $Na_2HPO_4$ than MEM. Phosphates easily tend to form ion pairs with chitosan, and, hence they can cause coagulation not only by charge compensation, but also by bridging mechanism [8]. Other electrolytes such as NaCl, $CaCl_2$ and $MgCl_2$ do affect the aggregation and re-stabilization of CS-based NCs along with the instability regions for each of the constituent cations [20]. In addition, lyotropic effects arising from the type and concentration of the occurring ions, particularly of negatively charged species, may also alter the hydration shell of the NC's surface, as suggested since the early studies conducted on surfactant micelles in the presence of various salts [25].

In previous works, lipophilic drugs, such as diazepam [1] or docetaxel [5], have effectively been associated to CS nanocapsules as they can easily be loaded at the oily core. In the present study, we have chosen capsaicin, due to its current and possible future pharmacological use for a number of therapies. Besides, its inclusion in a nanovehicle may provide a strategy to control its delivery during topical, transmucosal or intracellular delivery. The capacity of nanocapsules to entrap capsaicin allows anticipating the future utilization of these systems that may well benefit from the fundamental bioactive properties of CS (e.g. mucoadhesitivity) along with the potential to achieve prolonged release of the drug during topical or nasal administering.

As we have shown, CS's $M_w$ and DA determine the internal structure of the NC's shell, which in turn modulates the stability of the formulation under physiological conditions. Interestingly, CS's physicochemical properties also affected the EE of the formulation. As can be seen in Table 2, the highest EE was for those nanocapsules formulated with LDP-DA51, while it was reduced when the $M_w$ increased and/or the DA decreased. As we have shown in a previous study [8], CSs with low $M_w$ and high DA form more uniform and more hydrophilic shells than do CSs of lower DA and/or higher $M_w$. Hence, these results indicate that the characteristics of the CS shell of the NCs affect not only to the physical characteristics and colloidal stability under physiological conditions, but also the capacity of the nanocarrier formulation to efficiently encapsulate a lipophilic drug.

## Experimental

### Materials

A series of CS samples were prepared and purified from a parent batch of CS obtained from chitin sourced from squid pen supplied by Dr. Dominique Gillet of Mahtani Chitosan

Pvt Ltd (France). To this end, purified CS was depolymerized under nitrous acid generated from $NaNO_2$ to obtain two CS [26] batches of high and low degrees of polymerization ($M_w$ ~122 and 11 kDa, respectively, as determined by HPLC SEC-MALLS), here referred to as HDP CS and LDP CS, respectively. Portions of HDP CS and LDP CS samples were further *N*-acetylated under homogeneous conditions by adding the needed stoichiometric amount of acetic anhydride in 1,2-propanediol [27] so as to afford CS with DA values (determined by $^1$H nuclear magnetic resonance (NMR)) varying in the range 1.6 % to 56 % for HDP CS and 1.4 % to 51 % for LDP CS. A commercial CS sample of pharmaceutical grade, ChitopharmS® ($M_w$ ~279 kDa and DA ~20 % as certified by supplier), was a kind gift from Cognis GmbH (Düsseldorf, Germany) and was used without further purification; lecithin (Epikuron 145 V) was from Degussa (Spain); Miglyol 812® (caprylic/capric triglycerides) was supplied by Lemmel (Spain). Capsaicin (purity ≥99.0 %) was purchased from Sigma-Aldrich (Stenheim, Germany); all other reagents and solvents were of analytical or HPLC grade. Milli-Q quality water was used throughout.

*Preparation of nanocapsules* CS-based nanocapsules were prepared according with the protocol originally developed in our laboratory slightly modified by avoiding the use of poloxamer in the aqueous phase [1]. Briefly, 20 mg of lecithin were dissolved into 250 μL of ethanol, and then 62.5 μL of Miglyol 812® was added, followed by addition of 4.75 mL of acetone. Immediately afterwards, this organic phase was poured into of 10 mL of CS solution (0.5 mg/mL) in 5 % stoichiometric excess of acetic acid. Immediately upon addition of the organic phase into the aqueous CS solution, it turned milky. Acetone, ethanol and a portion of the volume of water were evaporated in a rotavapor at 40 °C for ~8 min to a final volume corresponding with one third of the original one. A nanoemuslion was prepared under an identical protocol as that used for CS NCs, but without including CS in the aqueous phase.

## Physical characterization

*Size and zeta potential* The size distribution of NCs was determined by PCS-NIBS (measurement angle 173°), and the zeta potential ($\zeta$) was measured by mixed laser Doppler velocimetry and phase analysis light scattering (M3–PALS), both using a Malvern Zetasizer NanoZS (Malvern Instruments, UK) fitted with a red laser light ($\lambda$=632.8 nm).

*Synchrotron SAXS* Measurements were carried out at the European Synchrotron Research Facility (Grenoble, France) at beamlineBM02. The following settings were utilized—$E$=14 kEv ($\lambda$=0.897 Å); sample-to-detector distance, 1.51 m. The collected scattering data were calibrated on the basis of the known positions of silver behenate powder Bragg reflections.

*Chitosan association* The net amount of CS associated with the NCs was measured indirectly by quantification of the concentration of the polymer remaining in the aqueous medium after separating the NCs by ultracentrifugation at 18,000 rpm for 1 h at 20 °C on a Beckman centrifuge Coulter Optima L-90 K (Fullerton, CA). To this end, the colorimetric assay based in the reaction of CS with Cibacron Brilliant Red 3B-A [28] was downscaled to a microplate assay.

*Transmission electron microscopy (TEM)* The ultrastructure of the various systems was probed on a Philips CM12 TEM instrument (Eindhoven, The Netherlands). To this end, 10 μL of a 2 % solution of phosphotungstic acid was mixed with an equal volume of a 1:100 dilution of nanocapsules in water. Immediately afterward, an aliquot of 5 μL was immobilized on a copper grid coated with a Formvar® membrane and allowed to dry.

*Drug encapsulation* To incorporate capsaicin into the NCs, an identical preparation procedure to the one described above was adopted but incorporating an accurately weighed amount of the drug (5 % load) dissolved in the ethanolic lecithin solution. The CS samples tested for this purpose were LDP-DA 1.4, LDP-DA 51 and ChitopharmS®. The EE of capsaicin was determined indirectly by calculating the difference between the total amount of capsaicin incorporated in the formulation and that determined remaining in the aqueous medium after separating the NCs by ultracentrifugation at 18,000 rpm for 1 h at 20 °C on a Beckman centrifuge Coulter Optima LK-90 K (USA). Capsaicin contents were determined by an HPLC-FLD method as described elsewhere [29].

*Stability in biological media* The colloidal stability of the developed NCs was investigated in the following cell culture media: (a) minimal essential medium Eagle (MEM M4655, Sigma-Aldrich) (pH 7.45), supplemented with 10 % (*v/v*) of fetal bovine serum (GIBCO-Invitrogen) and 1 % (*v/v*) of L-glutamine (Sigma-Aldrich), and 1 % (*v/v*) of penicillin/streptomycin solution (GPS, Sigma); (b) ECGM (PromoCell GmbH, Heidelberg) (pH 7.41) supplemented with 5 % (*v/v*) fetal calf serum (PromoCell GmbH, Heidelberg), 0.4 % (*v/v*) endothelial cell growth supplement/heparin (PromoCell GmbH, Heidelberg), 10 ng/mL epidermal growth factor (PromoCell GmbH, Heidelberg) and 1 μg/mL hydrocortisone (PromoCell GmbH, Heidelberg); (c) RPMI-1640 medium (PAA Laboratories GmbH) (pH 7.34) supplemented with 6 % (*v/v*) fetal bovine serum (PAA Laboratories

GmbH), 1 % (*v/v*) L-glutamine and 0.2 % (*v/v*) penicillin/streptomycin solution (GPS, Sigma-Aldrich). The stability was evaluated in terms of the evolution of the particle size distribution over time during incubation at 37 °C for up to ~48 h. Size measurements at given time intervals were registered by PCS-NIBS as described above.

## Conclusions

In summary, we have developed core–shell nanocapsules bearing an oily nucleus; a surfactant membrane and a hydrophilic polymer coat were obtained by spontaneous emulsification and stabilization by lecithin and accompanying interaction with CS of varying $M_w$ and DA. Electrostatic and also hydrophobic attractive forces are involved in the interaction between CS and lecithin as evidenced by the fact that, regardless of CS's DA, the particles retain most of the polysaccharide at their surface and their Z-average size does not vary much within the range ~140–200 nm. Their surface charge ($\zeta$), however, decreases as the DA increases beyond ~27 %. All the nanocapsule systems exhibited remarkable stability in MEM and ECGM cell culture media, and those bearing CSs of DA>27 % were stable also in RPMI-1640, which reflect the importance of hydration forces on the in vitro performance of these systems. Capsaicin, a currently established drug for pain therapy, was effectively encapsulated (72–96 %). The results of this work allow anticipating the promising potential of the design of CS-based NCs selecting the more appropriate polysaccharide's physicochemical properties in order to achieve the more efficient carrier.

**Acknowledgements** Support from the European Union for projects Nanobiosaccharides (ref. no. 013882 FP6) and BioNanoSmart-DDS (ref. no. 908111 FP7-PEOPLE Programme Marie Curie); from European Synchrotron Research Facility (France) for project ref. SC-2774; from "Ministerio de Ciencia e Innovación" (Spain) for project Consolider Nanobiomed (ref. no. CSD 2006–00012); from the "Consejería de Innovación, Ciencia y Tecnología de la Junta de Andalucía" (Spain) for projects P07-FQM-2496 and P07-FQM-03099 and from "Xunta de Galicia" (Spain) for a research fellowship to one of us (MJS) (Ángeles Alvariño research programme ref. IN840D) is in all cases gratefully acknowledged.

## References

1. Calvo P, Remuñan-Lopez C, Vila-Jato JL, Alonoso MJ (1997) Development of positively charged colloidal carriers: chitosan-coated polyester nanocapsules and submicron emulsions. Colloid Polymer Sci 275:46–53
2. Prego C, Fabre M, Torres D, Alonso MJ (2006) Efficacy and mechanism of action of chitosan nanocapsules for oral peptide delivery. Pharm Res 23(3):549–556
3. Prego C, Torres D, Alonso MJ (2006) Chitosan nanocapsules as carriers for oral peptide delivery: effect of chitosan molecular weight and type of salt on the in vitro behaviour and in vivo effectiveness. J Nanosci Nanotechnol 6(9–10):2921–2928
4. Prego C, Torres D, Alonoso MJ (2006) Chitosan nanocapsules: a new carrier for nasal peptide delivery. J Drug Deliv Sci Tech 16:331–337
5. Lozano MV, Torrecilla D, Torres D, Vidal A, Domínguez F, Alonso MJ (2008) Highly efficient system to deliver taxanes into tumor cells: docetaxel-loaded chitosan oligomer colloidal carriers. Biomacromolecules 9:2186–2193
6. Vicente S, Diaz B, Sanchez A, Gonzalez-Fernandez A, Alonso MJ Polysaccharide-based nanocapsules as vehicles for nasal immunization against hepatitis B. 2nd PharmSciFair, Premier European Platform for Advancing Pharmaceutical Sciences, 2010
7. López-Montilla JC, Herrera-Morales PE, Pandey S, Shah DO (2002) Spontaneous emulsification: mechanisms, physicochemical aspects, modeling, and applications. J Dispers Sci Technol 23:219–268
8. Santander-Ortega MJ, Peula-García JM, Goycoolea FM, Ortega-Vinuesa JL (2011) Chitosan nanocapsules: effect of chitosan molecular weight and acetylation degree on their electrokinetic and stability behaviour. Colloids Surf B Biointerfaces 82:571–580
9. Cortright DN, Zallasi A (2004) Biochemical pharmacology of the vanilloid receptor TRPV1. An update. Eur J Biochem 271:814–819
10. Bevan S, Szolcsányi J (1990) Sensory neuron-specific actions of capsaicin: mechanisms and applications. Trends Pharmacol Sci 11:330–333
11. Prego C, Garcia M, Torres D, Alonso MJ (2005) Transmucosal macromolecular drug delivery. J Contr Release 101(1–3):151–162
12. Calvo P, Vila-Jato JL, Alonso MJ (1997) Evaluation of cationic polymer-coated nanocapsules as ocular drug carriers. Int J Pharm 153:41–50, 41
13. Quemeneur F, Rammal A, Rinaudo M, Pepin-Donat B (2007) Large and giant vesicles "decorated" with chitosan: effects of pH, salt or glucose stress, and surface adhesion. Biomacromolecules 8:2512–2519
14. van der Lubben IM, Verhoef JC, Borchard G, Junginger HE (2001) Chitosan and its derivatives in mucosal drug and vaccine delivery. Eur J Pharm Sci 14:201–207
15. Quemeneur F, Rinaudo M, Pepin-Donat B (2008) Influence of molecular weight and ph on adsorption of chitosan at the surface of large and giant vesicles. Biomacromolecules 9:396–402
16. Fang N, Chan V (2003) Chitosan-induced restructuration of a mica-supported phospholipid bilayer: an atomic force microscopy study. Biomacromolecules 4:1596–1604
17. Fang N, Chan V, Mao HQ, Leong KW (2001) Interactions of phospholipid bilayer with chitosan: effect of molecular weight and pH. Biomacromolecules 2:1161–1168
18. Pavinatto FJ, Caseli L, Pavinatto A, dos Santos DS, Nobre TM, Zaniquelli MED, Silva HS, Miranda PB, de Oliveira ON (2007) Probing chitosan and phospholipid interactions using Langmuir and Langmuir-Blodgett films as cell membrane models. Langmuir 23:7666–7671
19. Nervo R, Konovalov O, Rinaudo M (2012) Chitosan-behenic acid monolayer interaction at the air-water interface: characterization of the adsorbed polymer layers by X-ray reflectivity. Int J Polymer Anal Char 17:11–20. doi:10.1080/1023666x.2011.628780
20. Santander-Ortega MJ, Lozano-Lopez MV, Bastos-Gonzalez D, Peula-Garcia JM, Ortega-Vinuesa JL (2009) Novel core–shell lipid-chitosan and lipid-poloxamer nanocapsules: stability by hydration forces. Colloid Polymer Sci 288:159–172
21. Alonso-Sande M, Cuna M, Remuñán-López C, Alonoso MJ (2006) Formation of new glucomannan-chitosan nanoparticles and study of their ability to associate and deliver proteins. Macromolecules 39:4152-4158
22. Santander-Ortega MJ, Jodar-Reyes AB, Csaba N, Bastos-Gonzalez D, Ortega-Vinuesa JL (2006) Colloidal stability of pluronic F68-

coated PLGA nanoparticles: a variety of stabilisation mechanisms. J Colloid Interface Sci 302:522–529
23. Santander-Ortega MJ, Stauner T, Loretz B, Ortega-Vinuesa JL, Bastos-Gonzalez D, Wenz G, Schaefer UF, Lehr CM (2010) Nanoparticles made from novel starch derivatives for transdermal drug delivery. J Contr Release 141:85–92
24. López-León T, Santander-Ortega MJ, Ortega-Vinuesa JL, Bastos-González D (2008) Hofmeister effects in colloidal systems: influence of the surface nature. J Phys Chem C 112:16060–16069
25. Anackearn EW, Ghose DHM (1963) Counterions and micelle size. I. Light scattering by solutions of dodecyltrimethylammonium salts. J Am Chem Soc 67:1713–1715
26. Allan GG, Peyron M (1995) Molecular weight manipulation of chitosan I: kinetics of depolymerization by nitrous acid. Carbohydr Res 277:257–272
27. Lamarque G, Lucas JL, Viton C, Domard A (2005) Physicochemical behavior of homogeneous series of acetylated chitosans in aqueous solution: role of various structural parameters. Biomacromolecules 6:131–146
28. Muzzarelli RAA (1998) Colorimetric determination of chitosan. Anal Biochem 260:255–257
29. Wang YY, Hong CT, Chiu WT, Fang JY (2001) In vitro and in vivo evaluations of topically applied capsaicin and nonivamide from hydrogels. Int J Pharm 224:89–104